

Gain Scheduled Active Steering Control Based on a Parametric Bicycle Model

S. Çağlar Başlamışlı, İlhan Polat and İ. Emre Köse

Abstract—This paper presents a gain scheduled active steering control design method to preserve vehicle stability in extreme handling situations. It is shown that instead of the classical linear tire model based on expressing cornering force proportional to tire sideslip angle, a simple rational model with validity extending beyond the linear regime of the tire may be considered. This results in a new formulation of the bicycle model in which tire sideslip angles and vehicle forward speed appear as time-varying parameters. Such a model happens to be useful in the design of controllers scheduled by tire sideslip angles: after having expressed the parametric bicycle model in the parametric descriptor form, a gain scheduled active steering controller is designed in this study to improve vehicle handling at “large” driver commanded steering angles. Simulations reveal the efficiency of the selected modeling and controller design methodology in enhancing vehicle handling capacity during cornering on roads with high and low adhesion coefficient.

I. INTRODUCTION

Vehicle dynamics modeling with uncertainties to deal with unknown parameters and nonlinear effects for active steering controller design has been occasionally treated in the literature. In [1], the saturation characteristics of rear tires were modeled by a linear function with uncertain rear cornering stiffness. H_∞ control theory was used to design a front wheel steering controller to guarantee robust stability. The designed controller was shown to work well on a nonlinear vehicle model, achieving robust stability and protecting the vehicle from spin. Later, Mammari et al. [2] obtained a linear fractional transformation (LFT) model of a bicycle model with nonlinear tire force generation formulation. The diagonal uncertainty matrix contained variations in vehicle speed, front and rear tire cornering stiffnesses. In [3], the uncertainties considered were vehicle mass, mass moment of inertia, road adhesion coefficient and an active steering control scheduled with speed variations was implemented so as to achieve robustness against uncertainties and good rejection of yaw moment disturbances.

We observed that driver commanded steering angles were kept at relatively small values in all of the above studies and that it was unclear how far tires were pushed to operate in the nonlinear regime in the simulations presented. Emphasis

This research was funded by Boğaziçi University Research Fund under Project No. 05A604. S. Çağlar Başlamışlı and İ. Emre Köse are with Department of Mechanical Engineering, Boğaziçi University, Bebek, Istanbul, 34342 Turkey {caglar.baslamisli, koseemre}@boun.edu.tr. İlhan Polat is with Delft Center for Systems and Control (DCSC), Delft University of Technology, Delft, The Netherlands, i.polat@tudelft.nl

was rather put on improving vehicle handling on roads with low adhesion coefficient at small driver commanded steering angles. Tire saturation was only partially taken into account during controller synthesis in studies cited above. For the purpose of active steering design, these lead one to seek a tire model formulation simple enough to be used in onboard computer algorithms but complete enough to display such features as tire force saturation, load and brake force variation effects.

Among available nonlinear tire models, the Magic Formula (MF) [7] is formulated through such a large number of constants and the formulation is so nonlinear that its usage for vehicle dynamics controller (VDC) synthesis is limited. Lately, the work of Gerdes et al [4] on determining the stability margins provided by an active steering controller encompassed fitting a rational function to the nonlinear HSRI [5] tire model and has inspired our own work in fitting a rational function to MF.

This paper is organized as follows. In the first part of the paper, several modifications to be incurred on the bicycle model so as to reflect saturating tire behavior at large tire slip angles are presented. In Section II, rational fits are obtained for MF under various loading, road adhesion and combined slip conditions. This leads to a parametric description of the bicycle model formulation in which vehicle speed and tire sideslip angles appear as the varying parameters. A gain scheduled active steering controller design method based on a parametric descriptor formulation of the previous model is presented in Section III. In Section IV, performance of the proposed active steering controller during extreme cornering is presented. Performances of scheduled and static controllers are compared. Robustness against road adhesion coefficient is evaluated. Finally, conclusions are presented in Section V.

II. TIRE MODELING WITH RATIONAL FUNCTION AND PARAMETRIC DESCRIPTOR FORMULATION OF BICYCLE MODEL

A. Tire Cornering Force Fitting Model with Rational Function

Tires tend to operate in the nonlinear regime in an extreme handling situation. Hence, the advantages of using a tire model with validity extending over a large range of tire slip angle are worth investigating. We consider a rational function expressed as:

$$F_y = \frac{p_1\alpha + p_2}{\alpha^2 + q_1\alpha + q_2} \quad (1)$$

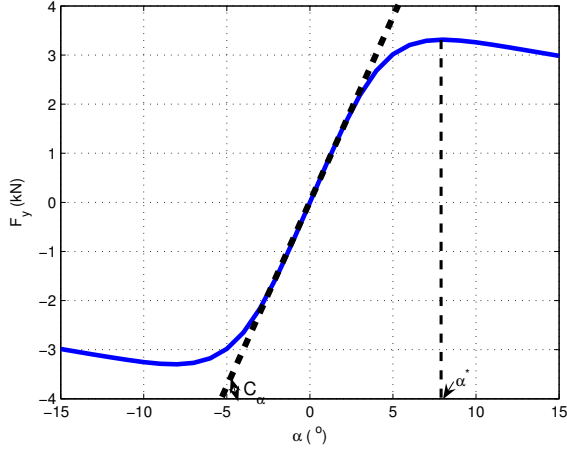


Fig. 1. Generic Lateral Tire Force vs Slip Angle obtained by the Magic Formula

in order to approximate the nonlinear MF formulation given for pure lateral slip:

$$F_{y0} = D_y \sin \left(C_y \arctan \left[B_y (1 - E_y) \alpha + E_y \arctan (B_y \alpha) \right] \right) \quad (2)$$

where B_y , C_y , D_y and E_y are experimental constants. It is possible to propose polynomials of higher degrees at the numerator and denominator of (1) for more accurate modeling but this would render the ensuing controller design more complex. Several relationships between coefficients are readily available (Figure 1):

- $\frac{p_1}{q_2} \approx C_\alpha$, the tire cornering stiffness;
- as the tire cornering force is an odd function of tire slip angle, one possibility is to have $p_2 \approx 0$ and $q_1 \approx 0$;
- as the maximum cornering force occurs at α^* , one must have $\frac{dF_y}{d\alpha} = 0$ at α^* .

With the above observations, (1) becomes:

$$F_y = \frac{C_\alpha \alpha}{\left(\frac{\alpha}{\alpha^*}\right)^2 + 1} \quad (3)$$

Denoting $\gamma_\alpha = \left(\frac{1}{\alpha^*}\right)^2$, one can conceive γ_α as a shape factor for the model and better fits may be obtained by varying γ_α and C_α around their nominal values. Next, we assume that cornering force variation is proportional to the product of combined variations in road adhesion coefficient and normal load. We take $\gamma_z \frac{\mu F_z}{\mu_o F_{z0}}$, where μ_o stands for the nominal road adhesion coefficient and F_{z0} stands for the nominal tire load, as a factor multiplying (3) to account for simultaneous variations in road adhesion and normal load. Furthermore, Pacejka et al [7] proposed to multiply the cornering force obtained for pure lateral slip by a weighing factor $G_{y\lambda}$ in order to represent combined slip conditions:

$$G_{y\lambda} = \cos \left(C_{y\lambda} \arctan \left\{ B_{y\lambda} \lambda - E_{y\lambda} [B_{y\lambda} \lambda - \arctan(B_{y\lambda} \lambda)] \right\} \right) (G_{y\lambda o})^{-1} \quad (4)$$

where

$$G_{y\lambda o} = \cos \left(C_{y\lambda} \arctan \left\{ B_{y\lambda} S_{Hy\lambda} - E_{y\lambda} [B_{y\lambda} S_{Hy\lambda} - \arctan(B_{y\lambda} S_{Hy\lambda})] \right\} \right) \quad (5)$$

and where λ stands for longitudinal slip and where $B_{y\lambda}$, $C_{y\lambda}$, $E_{y\lambda}$ and $S_{Hy\lambda}$ are experimental constants. It is possible to approximate $G_{y\lambda}$ by $\frac{1}{\left(\frac{\lambda}{\lambda^*}\right)^2 + 1}$, where λ^* corresponds roughly to the point of inflection of $G_{y\lambda}$. Again, we can define $\gamma_\lambda = \left(\frac{1}{\lambda^*}\right)^2$ as a shape factor to obtain better fits.

To sum up, the following rational function is proposed for the approximation of lateral force under combined slip conditions:

$$F_y(\alpha, \lambda, \mu, F_z) \approx \frac{\mu F_z}{\mu_o F_{z0}} \frac{\gamma_z}{\gamma_\lambda \lambda^2 + 1} \frac{C_\alpha}{\gamma_\alpha \alpha^2 + 1} \alpha \quad (6)$$

B. A Parametric Bicycle Model

Nonlinear equations of motion for the bicycle model are given by:

$$m(\dot{v} + ur) = F_{yf} + F_{yr} \quad (7a)$$

$$J\dot{r} = aF_{yf} - bF_{yr} \quad (7b)$$

where v is the lateral speed, u is the longitudinal speed, r is the yaw rate, F_{yf} is the front axle cornering force and F_{yr} is the rear axle cornering force. The usual procedure in deriving a linear model is to replace axle cornering force expressions by $C_\alpha \alpha$, hence making a linear tire model assumption. In this paper, it is proposed to make use of (6) while doing substitutions under the following assumptions:

- Front tires share the tire cornering stiffness $\frac{C_f}{2}$ where C_f is the front axle cornering stiffness that appears in the classical linear bicycle model. Similarly, rear tires share the tire cornering stiffness $\frac{C_r}{2}$.
- Longitudinal speed is much greater than lateral speed hence longitudinal speed u is nearly equal to total vehicle speed U .
- Front tires share the common slip angle $\alpha_f = \delta - \beta - \frac{ar}{u}$ and rear tires share the common slip angle $\alpha_r = -\beta + \frac{br}{u}$ [6].

At this stage, it is possible to express front and rear axle lateral forces as:

$$F_{yf} = \frac{\mu C_f \alpha_f}{2\mu_o F_{zf0}} \left(\frac{1}{\gamma_{\lambda 1} \lambda_1^2 + 1} \frac{\gamma_{z1} F_{z1}}{\gamma_{\alpha 1} \alpha_f^2 + 1} + \frac{1}{\gamma_{\lambda 2} \lambda_2^2 + 1} \frac{\gamma_{z2} F_{z2}}{\gamma_{\alpha 2} \alpha_f^2 + 1} \right) \quad (8a)$$

$$F_{yr} = \frac{\mu C_r \alpha_r}{2\mu_o F_{zr0}} \left(\frac{1}{\gamma_{\lambda 3} \lambda_3^2 + 1} \frac{\gamma_{z3} F_{z3}}{\gamma_{\alpha 3} \alpha_r^2 + 1} + \frac{1}{\gamma_{\lambda 4} \lambda_4^2 + 1} \frac{\gamma_{z4} F_{z4}}{\gamma_{\alpha 4} \alpha_r^2 + 1} \right) \quad (8b)$$

Then, the following simplifications are made:

- Longitudinal slip terms are taken as zero hence assuming pure cornering.
- Road adhesion coefficient is taken as μ_o hence assuming driving on dry road.
- When considered as uncertain parameters, shape factors γ_{α_i} and γ_{z_i} can be merged into a single factor γ_{α} ,

which can be optimized at a later stage by comparing responses of nonlinear and parametric vehicle models.

Under the above assumptions, the following parametric bicycle model is obtained:

$$\dot{\beta} = -\frac{C_f^* + C_r^*}{mU}\beta + \left[-1 + \frac{-aC_f^* + bC_r^*}{mU^2} \right] r + \frac{C_f^*}{mU}\delta \quad (9a)$$

$$\dot{r} = \frac{-aC_f^* + bC_r^*}{J}\beta - \frac{a^2C_f^* + b^2C_r^*}{JU}r + \frac{aC_f^*}{J}\delta \quad (9b)$$

where $C_f^* = \frac{C_f}{\gamma_\alpha \alpha_f^2 + 1}$ and $C_r^* = \frac{C_r}{\gamma_\alpha \alpha_r^2 + 1}$. One should note that $\beta = \arctan(\frac{v}{u}) \approx \frac{v}{u}$ has been taken while deriving (9) from (7). The simulation displayed in Figure 2 has been obtained by taking $\gamma_\alpha = 35$ and using a two-track nonlinear vehicle model described in more detail in Section IV-A. At large steering angle, it is observed that responses of the classical bicycle model do not predict anymore responses of the nonlinear vehicle model. However, responses of the parametric bicycle model are in good agreement with those of the nonlinear vehicle model.

III. GAIN-SCHEDULED ACTIVE STEERING CONTROL

A natural source of parameter dependence is the quasi-linearization of nonlinear systems. By treating nonlinear state-dependent terms as varying parameters of the system, a wide class of nonlinear systems can be modeled as linear parameter varying (LPV) systems, which is the case for parametric bicycle model considered in this study.

A. Dynamic Output Feedback Controller Synthesis via Parametric Descriptor Form

An LPV system in the descriptor form is given as follows:

$$\begin{aligned} E_x(r)\dot{x} &= A(r)x + B_1(r)w + B_2(r)u \\ z &= C_1(r)x + D_{11}(r)w + D_{12}(r)u \\ y &= C_2(r)x + D_{21}(r)w \end{aligned} \quad (10)$$

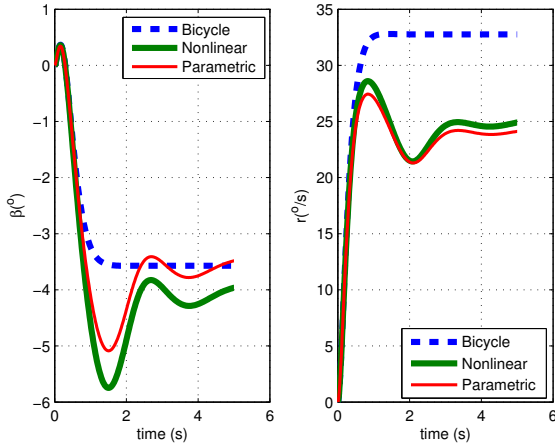


Fig. 2. Vehicle response for driver's large step input ($\delta = 5^\circ$)

where x is the state vector, w the external disturbance, u the control input and z and y are the controlled and measured outputs, respectively. The vector dimensions are as follows: $x(t) \in \mathbb{R}^n$, $w(t) \in \mathbb{R}^{m_1}$, $u(t) \in \mathbb{R}^{m_2}$, $z(t) \in \mathbb{R}^{p_1}$ and $y(t) \in \mathbb{R}^{m_2}$. We assume that all system matrices are affine in the parameter vector $r : \mathbb{R} \rightarrow \mathbb{R}^q$. The admissible parameter trajectories are continuously differentiable time-varying vectors such that: $r(t) \in \mathcal{R}$ and $\dot{r}(t) \in \mathcal{D}$ for all $t \geq 0$, where

$$\mathcal{R} := \{r \in \mathbb{R}^q : \underline{r}_\alpha \leq r_\alpha \leq \bar{r}_\alpha \quad \forall \alpha = 1 : q\} \quad \text{and}$$

$$\mathcal{D} := \{d \in \mathbb{R}^q : \underline{\dot{r}}_\alpha \leq \dot{r}_\alpha \leq \bar{\dot{r}}_\alpha \quad \forall \alpha = 1 : q\}.$$

The set of admissible parameter trajectories are defined as follows:

$$\mathcal{P} := \{r : \mathbb{R} \rightarrow \mathbb{R}^q : r(t) \in \mathcal{R} \text{ and } \dot{r}(t) \in \mathcal{D} \quad \forall t \geq 0\}.$$

For the LPV system in the general descriptor form (10), it is aimed in this section to design a controller of the form

$$\begin{aligned} \dot{x}_c &= A_c(r)x_c + B_c(r)y \\ u &= C_c(r)x_c \end{aligned} \quad (11)$$

such that the closed-loop system is asymptotically stable with L_2 -gain γ .

Theorem 3.1: [10] Assume that:

$$\begin{bmatrix} -\gamma I & D_{11}^T \\ D_{11} & -\gamma I \end{bmatrix} \prec 0 \quad \forall r \in \mathcal{R}. \quad (12)$$

Then, there exists a controller of the form (11) that asymptotically stabilizes system (10) if there exist $X(r) = \bar{X}(r)^T \in \mathbb{R}^{n \times n}$, $Y(r) = \bar{Y}(r)^T \in \mathbb{R}^{n \times n}$, $F(r) \in \mathbb{R}^{m_2 \times n}$ and $G(r) \in \mathbb{R}^{n \times p_2}$ such that

$$\begin{bmatrix} AX E_x^T + E_x X A^T + B_2 F E_x^T & & & \\ + E_x F^T B_2^T - E_x \dot{X} E_x^T & * & * & \\ B_1^T & -\gamma I & * & \\ C_1 X E_x^T + D_{12} F E_x^T & D_{11} & -\gamma I & \end{bmatrix} \prec 0 \quad \forall (r, \dot{r}) \in \mathcal{R} \times \mathcal{D} \quad (13)$$

$$\begin{bmatrix} A^T Y E_x + E_x^T Y A + G C_2 + C_2^T G^T & & & \\ + \dot{E}_x^T Y E_x + E_x^T \dot{Y} E_x + E_x^T Y \dot{E}_x & * & * & \\ B_1^T Y E_x + D_{21}^T G^T & -\gamma I & * & \\ C_1 & D_{11} & -\gamma I & \end{bmatrix} \prec 0 \quad \forall (r, \dot{r}) \in \mathcal{R} \times \mathcal{D} \quad (14)$$

$$\begin{bmatrix} X(r) & I \\ I & E_x(r)^T Y(r) E_x(r) \end{bmatrix} \succ 0 \quad \forall r \in \mathcal{R}. \quad (15)$$

In this case, the controller in (11) can be given by the following definitions

$$D_c = 0 \quad C_c(r) = F X^{-1} \quad B_c(r) = -Z^{-1} G \quad (16a)$$

$$\begin{aligned} A_c(r, \dot{r}) &= Z^{-1} A^T E^{-T} X^{-1} + Z^{-1} E_x^T Y [A + B_2 C_c] \\ &\quad - B_c C_2 + Z^{-1} L X^{-1} + Z^{-1} X^{-1} \dot{X} X^{-1} \end{aligned} \quad (16b)$$

where $Z(r) = E_x(r)^T Y(r) E_x(r) - X(r)^{-1} \succ 0$ and

$$L = \begin{bmatrix} E^T Y B_1 + G D_{21} & C_1^T \\ & \begin{bmatrix} -\gamma I & D_{11}^T \\ D_{11} & -\gamma I \end{bmatrix}^{-1} \\ & \begin{bmatrix} B_1^T E_x^{-T} \\ C_1 X \end{bmatrix} \end{bmatrix}$$

In (13) and (14), the parameter dependence is omitted to simplify the notation.

From (13) - (15), the sign definiteness of the given LMIs must be validated at each point of $\mathcal{R} \times \mathcal{D}$, hence infinite dimensional solvability conditions are obtained. The satisfaction of (13), (14) and (15) over $\mathcal{R} \times \mathcal{D}$ can be guaranteed by checking the vertices $\mathcal{R}_{vex} \times \mathcal{D}_{vex}$, provided that the second derivatives with respect to each parameter are positive semidefinite [8],[10].

B. Application to Active Steering Control Design

1) *Design objective and reference signals:* The aim of the active steering controller during cornering is two-fold: keeping the body sideslip angle as low as possible and tracking a reference yaw rate. The yaw rate reference is constructed based on the yaw rate response $r_{lin}(t)$ of a linear bicycle model having similar tire cornering characteristics in the linear operation range of tires and is saturated by the physical limit imposed by the current road adhesion coefficient ($|r_{max}| \leq |\frac{\mu g}{U}$). Hence,

$$r_{ref}(t) = \min \left\{ \left| \frac{\mu g}{U} \text{sign}(\delta(t)), r_{lin}(t) \right\} \quad (17)$$

where $r_{lin}(t)$ is obtained from

$$r_{lin}(s) = -\frac{(a+b)C_f C_r U}{C_f C_r (a+b)^2 + mU^2(bC_r - aC_f)} \frac{1}{1 + T_e s} \delta(s), \quad (18)$$

and where T_e is a design time constant [11].

2) *Parametric descriptor form of bicycle model:* Given the above arguments, three kinds of disturbances are observed to act on the system: driver commanded steering angle δ , sideslip angle reference β_{ref} and yaw rate reference r_{ref} . The only control input is active steering correction. Measured and controlled outputs are both taken as sideslip angle and yaw rate errors, implying $C_1 = I_2 = C_2$, $D_{11} = \begin{bmatrix} 0 & -1 & 0 \\ 0 & 0 & -1 \end{bmatrix} = D_{21}$, $D_{12} = 0$. Controller design is undertaken after a simple manipulation of (9) that yields the following parametric descriptor form:

$$E_x(r) = E_0 + r_1 E_2 + r_2 E_2 + r_3 E_3 \quad (19a)$$

$$A(r) = A_0 + r_1 A_1 + r_2 A_2 + r_3 A_3 \quad (19b)$$

$$B_1(r) = B_{10} + r_1 B_{11} + r_2 B_{12} + r_3 B_{13} \quad (19c)$$

$$B_2(r) = B_{20} + r_1 B_{21} + r_2 B_{22} + r_3 B_{23} \quad (19d)$$

Here, $r_1 = \alpha_f^2$, $r_2 = \alpha_r^2$ and $r_3 = (\alpha_f \alpha_r)^2$ naturally appear as scheduling parameters.

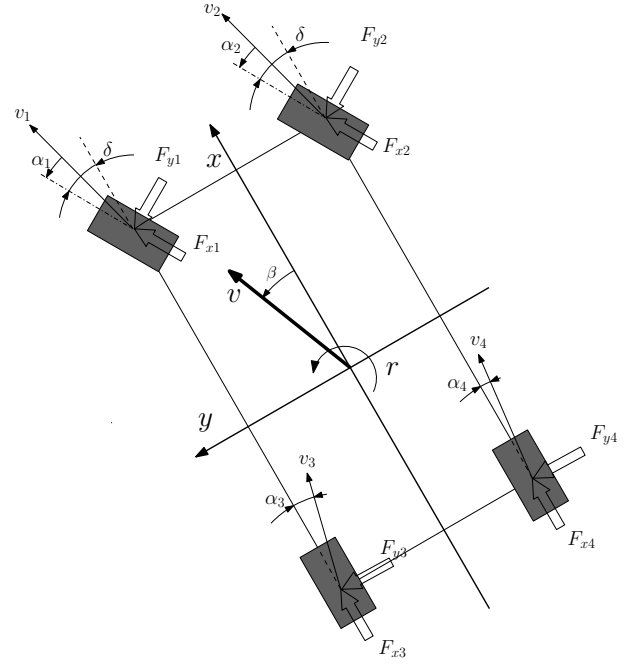


Fig. 3. Nonlinear two-track yaw plane vehicle model

3) *Controller design strategy:* Two controllers have been finally computed:

- While designing K_1 , $\gamma_\alpha = 35$ has been assumed, to account for tire saturation in controller synthesis.
- While designing K_2 , $\gamma_\alpha = 0$ has been taken, hence assuming linear tire behavior during controller synthesis.

For the tire model used in this research, F_y can be assumed to vary in the range $(0 - 8000 N)$. The linear regime of tires has been analyzed to extend up to $0.14 rad \approx 8^\circ$ under all operating conditions (changes in road adhesion, lateral weight transfer, combined slip). Assuming a slight excursion into the nonlinear region, we assume an upper limit of 10° for both front and rear tire sideslip angle. Under the light of these observations, the problem has been solved with $0 \leq r_1 \leq (10 \times \frac{\pi}{180})^2$, $0 \leq r_2 \leq (10 \times \frac{\pi}{180})^2$, $0 \leq r_3 \leq (10 \times \frac{\pi}{180})^4$. Furthermore, taking $-1 \leq \dot{r}_1 \leq 1$, $-1 \leq \dot{r}_2 \leq 1$ and $-1 \leq \dot{r}_3 \leq 1$ has been observed to yield quite satisfactory results. Nominal vehicle speed has been taken as $v_o = 20 m/s$. Speed variations are expected to be small when implementing active steering control.

IV. NONLINEAR SIMULATION MODEL AND SIMULATION RESULTS

A. Nonlinear Simulation Model

The nonlinear simulation model taken from [6] includes states which are essential for vehicle dynamics control (Figure 3). These are vehicle speed U , vehicle body sideslip angle β and yaw rate r . Longitudinal dynamics, lateral dynamics and yaw dynamics are respectively given by:

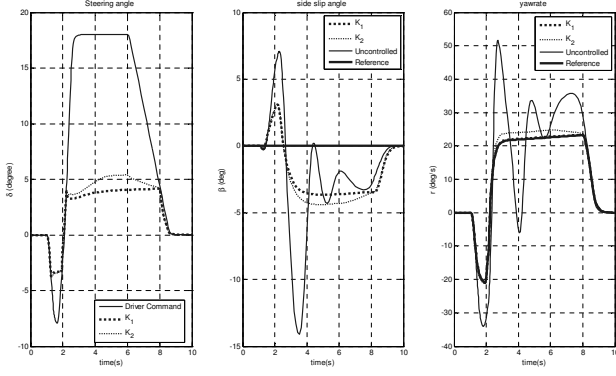


Fig. 4. Active steering controller performance on dry road ($\mu = 1$) for “small” driver commanded steering angle

$$\dot{U} = \frac{1}{m} \left((F_{x1} + F_{x2}) \cos(\beta - \delta) + (F_{x3} + F_{x4}) \cos \beta + (F_{y1} + F_{y2}) \sin(\beta - \delta) + (F_{y3} + F_{y4}) \sin \beta \right), \quad (20)$$

$$\dot{\beta} = \frac{1}{mU} \left(-(F_{x1} + F_{x2}) \sin(\beta - \delta) - (F_{x3} + F_{x4}) \sin \beta + (F_{y1} + F_{y2}) \cos(\delta - \beta) + (F_{y3} + F_{y4}) \cos \beta \right) - r, \quad (21)$$

$$\dot{r} = \frac{1}{J_z} \left(F_{x1} \left(a \sin \delta - \frac{T}{2} \cos \delta \right) + F_{x2} \left(a \sin \delta + \frac{T}{2} \cos \delta \right) + \frac{T}{2} (F_{x4} - F_{x3}) + F_{y1} \left(\frac{T}{2} \sin \delta + a \cos \delta \right) + F_{y2} \left(-\frac{T}{2} \sin \delta + a \cos \delta \right) - b(F_{y3} + F_{y4}) \right). \quad (22)$$

Tire forces F_x and F_y depend on both tire sideslip angles and tire longitudinal slips in combined slip conditions. The formulation of tire forces is based on MF.

B. Simulation Results

1) *Simulation 1*: Results for a fishhook maneuver with maximum driver commanded steering angle $\delta = 18^\circ$ carried out on dry road are shown in Figure 4. Responses of controlled vehicles are satisfactory as displayed by the sideslip angle and yaw rate curves, K_1 resulting in better yaw rate tracking and lower vehicle sideslip angle response than K_2 . The action of active front steering control has a tendency of decreasing the commanded steering angle under the value resulting in marginal vehicle stability ($\approx 5^\circ$). Parameter variations during these maneuvers can be observed in Figure 5. Parameter bounds are relatively well satisfied. It is noted that vehicle speed changes slightly during the maneuver which justifies the constant speed assumption made during controller synthesis.

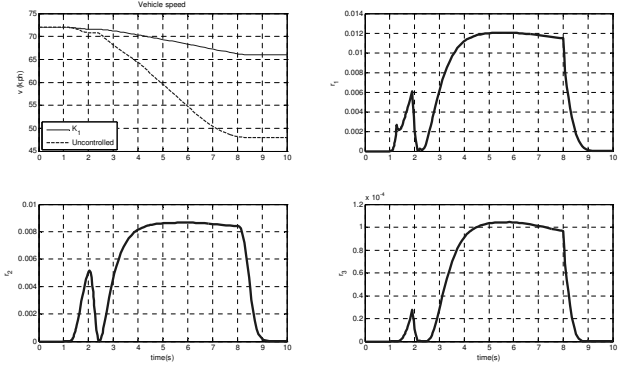


Fig. 5. Parameter variation on dry road ($\mu = 1$) for “small” driver commanded steering angle

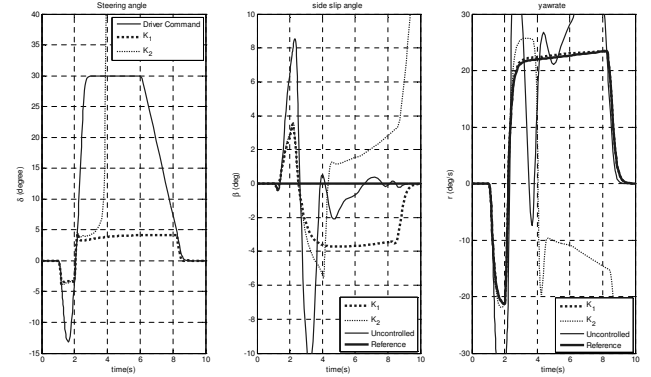


Fig. 6. Active steering controller performance on dry road ($\mu = 1$) for “large” driver commanded steering angle

2) *Simulation 2*: In a second series of simulations, performances of K_1 and K_2 at large driver commanded steering angles are investigated. Results for a fishhook maneuver with driver commanded steering angle as large as $\delta = 30^\circ$ carried out on dry road are shown in Figure 6. This time K_2 is unable to stabilize the vehicle and results in a performance that is even worse than uncontrolled vehicle performance, while K_1 still results in good yaw rate tracking and acceptable sideslip angle response. Parameter variations during these maneuvers can be observed in Figure 7. Parameter bounds are again well satisfied.

3) *Simulation 3*: In a third series of simulations, performances of K_1 and K_2 are investigated for cornering maneuvers on roads with low adhesion ($\mu = 0.5$). Inspection of Figure 8 and Figure 9 again shows that K_1 can stabilize vehicle response for “large” driver commanded steering angles and relatively low road adhesion coefficient achieving nicely damped vehicle response, while the uncontrolled vehicle is seen to display highly oscillatory dynamics and while K_2 results in even poorer response.

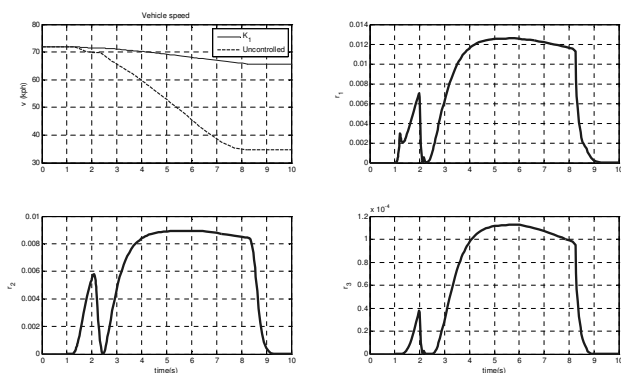


Fig. 7. Parameter variation on dry road ($\mu = 1$) for "large" driver commanded steering angle

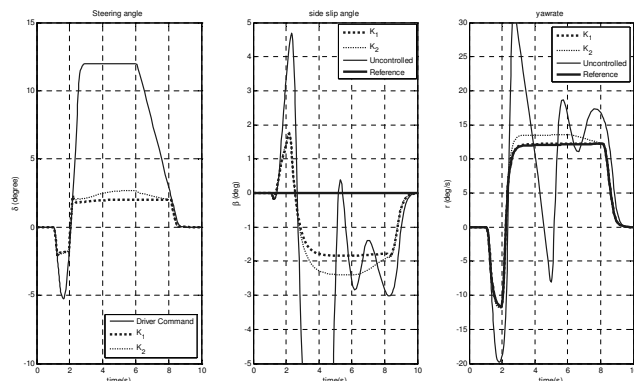


Fig. 8. Active steering controller performance on wet road ($\mu = 0.5$) for small driver commanded steering angle

V. DISCUSSION OF RESULTS AND CONCLUSION

Major contributions of this paper consist of the proposed rational tire model, the parametric descriptor representation of the bicycle model and the gain scheduled active steering controller design based on this representation. It has been shown that instead of the classical linear tire model based on expressing cornering force proportional to tire sideslip angle, a simple rational model with validity extending beyond the linear regime of the tire may be considered. This has resulted in a new formulation of the bicycle model in which tire slip angles and vehicle forward speed have appeared as changing parameters. Then, after having expressed the modified bicycle model in the parametric descriptor form, a gain scheduled active steering controller has been designed.

Two different controllers have been considered. The controller synthesized by taking tire saturation into account has been observed to result in good vehicle response for large driver commanded steering angle maneuvering on both dry and slippery road. Meanwhile, the controller synthesized based on the classical bicycle model (hence neglecting cornering force saturation) has resulted in poor response for large driver commanded steering angle.

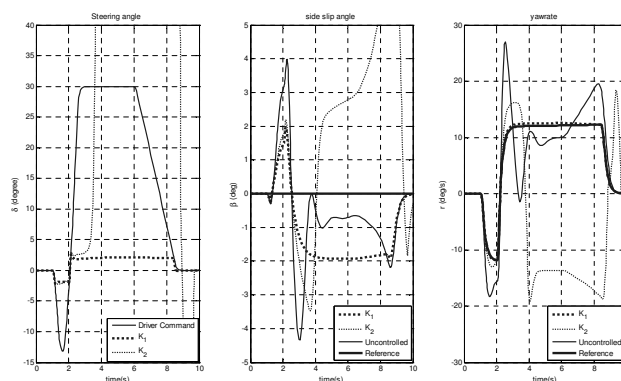


Fig. 9. Active steering controller performance on wet road ($\mu = 0.5$) for large driver commanded steering angle

VI. ACKNOWLEDGMENTS

The third author acknowledges support of the European Union Framework Programme 6 through the AUTOCOM SSA project (INCO Project No: 1642).

REFERENCES

- [1] Ono, E., Hosoe, S., Tuan, H.D. and Doi, S., "Bifurcation in Vehicle Dynamics and Robust Front Wheel Steering Control", IEEE Transactions on Control Systems Technology, Vol.6, No.3, 1998.
- [2] Mammari, S. and Koenig, D., "Vehicle Handling Improvement by Active Steering", Vehicle System Dynamics, V.38, No.3, pp 211-242, 2002.
- [3] Hecker, S., "Robust Hinf-based Vehicle Steering Control Design", IEEE International Conference on Control Applications, Munich, Germany, Proceeding of IEEE CCA, 2006.
- [4] Switkes, J. and Gerdes, C., "Guaranteeing Lanekeeping Performance with Tire Saturation Using Computed Polynomial Lyapunov Functions", Proceedings of IMECE, ASME International Mechanical Engineering Congress and Exposition Orlando, Florida, USA, 2005.
- [5] Dugoff, H., Francher, P.S. and Segel, L., "An Analysis of Tire Traction Properties and Their Influence on Vehicle Dynamic Performance", SAE paper No. 700377, 1977.
- [6] Kiencke, U. and Nielsen, L., "Automotive Control Systems For Engine, Driveline and Vehicle", Springer, 2000.
- [7] Bakker, E., Nyborg, L. and Pacejka, H.B., "Tyre Modeling for Use in Vehicle Dynamics Studies", SAE paper No. 870421, 1987.
- [8] Gahinet, P., Apkarian, P. and Chilali, M., "Affine Parameter-Dependent Lyapunov Functions for Real Parametric Uncertainty", IEEE Transactions on Automatic Control, Vol.41, No.3, pp.436-442, 1996.
- [9] Scherer, C.W., Gahinet, P. and Chilali, M., "Multiobjective Output-Feedback via LMI Optimization", IEEE Transactions on Automatic Control, Vol.42, No.7, pp.896-911, 1997.
- [10] Polat, İ., Eşkinat E. and Köse İ.E., "Dynamic Output Feedback Control of Quasi-LPV Mechanical Systems", to appear in IET Control Theory & Applications
- [11] Dixon, J., "Tires, suspension and Handling", Second Edition, 1992.

Nomenclature:

m : Vehicle mass, 1987 kg; a : Distance from vehicle center of gravity to front axle, 1.14 m; b : Distance from vehicle center of gravity to rear axle, 1.43 m; T : Vehicle track, 1.86 m; J_z : Vehicle moment of inertia, 4510 kgm²; C_f : Front axle cornering stiffness, 108000 N; C_r : Rear axle cornering stiffness, 98000 N.